

Current Biology

The oral microbiota of wild bears in Sweden reflects the history of antibiotic use by humans

Highlights

- Wild animals can be used as indicators of antibiotic contamination of environments
- Bear oral microbiota from the pre-antibiotic era reveal a baseline of natural AMR
- Bear AMR load tracked human antibiotic use over the last 80 years
- Bear AMR load decreased after Swedish strategy to curb AMR was implemented

Authors

Jaelle C. Brealey, Henrique G. Leitão, Thijs Hofstede, Daniela C. Kalthoff, Katerina Guschanski

Correspondence

jaelle.brealey@ntnu.no (J.C.B.),
katerina.guschanski@ebc.uu.se (K.G.)

In brief

Using oral microbiomes preserved in dental calculus of wild brown bear specimens from the last 180 years, Brealey et al. track human-associated antimicrobial resistance (AMR) in the environment and show that it correlates with human antibiotic use in Sweden. Encouragingly, national control policies to curb AMR show a positive effect.



Report

The oral microbiota of wild bears in Sweden reflects the history of antibiotic use by humans

Jaelle C. Brealey,^{1,4,5,*} Henrique G. Leitão,¹ Thijs Hofstede,¹ Daniela C. Kalthoff,² and Katerina Guschanski^{1,3,6,7,*}

¹Department of Ecology and Genetics/Animal Ecology, Uppsala University, Norbyvägen 18D, Uppsala 75236, Sweden

²Department of Zoology, Swedish Museum of Natural History, PO Box 50007, Stockholm 10405, Sweden

³Institute of Evolutionary Biology, School of Biological Sciences, University of Edinburgh, Ashworth Laboratories, The Kings Buildings, Charlotte Auerbach Road, Edinburgh EH9 3FL, UK

⁴Present address: Department of Natural History, NTNU University Museum, Trondheim, Norway

⁵Twitter: @JaeBrealey

⁶Twitter: @kguschan

⁷Lead contact

*Correspondence: jaelle.brealey@ntnu.no (J.C.B.), katerina.guschanski@ebc.uu.se (K.G.)

<https://doi.org/10.1016/j.cub.2021.08.010>

SUMMARY

Following the advent of industrial-scale antibiotic production in the 1940s,¹ antimicrobial resistance (AMR) has been on the rise and now poses a major global health threat in terms of mortality, morbidity, and economic burden.^{2,3} Because AMR can be exchanged between humans, livestock, and wildlife, wild animals can be used as indicators of human-associated AMR contamination of the environment.⁴ However, AMR is a normal function of natural environments and is present in host-associated microbiomes, which makes it challenging to distinguish between anthropogenic and natural sources.^{4,5} One way to overcome this difficulty is to use historical samples that span the period from before the mass production of antibiotics to today. We used shotgun metagenomic sequencing of dental calculus, the calcified form of the oral microbial biofilm, to determine the abundance and repertoire of AMR genes in the oral microbiome of Swedish brown bears collected over the last 180 years. Our temporal metagenomics approach allowed us to establish a baseline of natural AMR in the pre-antibiotics era and to quantify a significant increase in total AMR load and diversity of AMR genes that is consistent with patterns of national human antibiotic use. We also demonstrated a significant decrease in total AMR load in bears in the last two decades, which coincides with Swedish strategies to mitigate AMR. Our study suggests that public health policies can be effective in limiting human-associated AMR contamination of the environment and wildlife.

RESULTS

Animals and their associated microbiomes are increasingly recognized as sources of potential human pathogens, including bacteria that carry antimicrobial resistance (AMR).⁶ Antibiotics and resistant bacteria from human healthcare and agricultural settings leak into the environment through waste production,^{7–10} where wildlife can come into contact with contaminated soil, water, and food sources.¹¹ Evidence exists for transfer of resistant bacteria between wildlife, domestic animals, and humans,¹² for example, via flies and wild birds co-inhabiting with livestock.^{13–15} Furthermore, AMR is ubiquitous in nature, either as defense against the antibiotics naturally produced by some bacteria and fungi¹⁶ or as a byproduct of general detoxifying functions.¹⁷ Accordingly, antibiotic resistance genes (ARGs) have been found across the globe, including in the most pristine environments free from human activities.^{18–20} It can therefore be difficult to establish a natural, human-unaffected AMR baseline and to distinguish between human-associated and natural sources of AMR.^{4,5}

Historical samples that predate industrial-scale antibiotic production offer an opportunity to characterize natural levels of

environmental AMR. Focusing on host microbiomes is particularly important, as these microbial communities are associated with eukaryotes and are therefore more relevant than free-living environmental microbiomes for understanding AMR dynamics with importance to humans. However, most host microbiomes are not preserved after host death. One exception is dental calculus, the calcified form of the dental plaque microbial biofilm that forms on mammalian teeth.²¹ It is built up periodically throughout an individual's life and preserves DNA from the oral microbiome within a calcified matrix, protected from invasion by external microorganisms.^{22,23} Metagenomic sequencing of dental calculus samples has detected ARGs in medieval humans²³ and 19th–20th century wild animals,²⁴ thus suggesting that this material can be used to trace AMR dynamics through time.

We studied the temporal progression of AMR in host-associated microbiomes of wild brown bears (*Ursus arctos*) in Sweden, by characterizing the abundance and repertoire of ARGs from bear dental calculus (Figure 1). We have previously shown that metagenomic sequences from dental calculus are a rich source of information on the oral microbial community of non-human



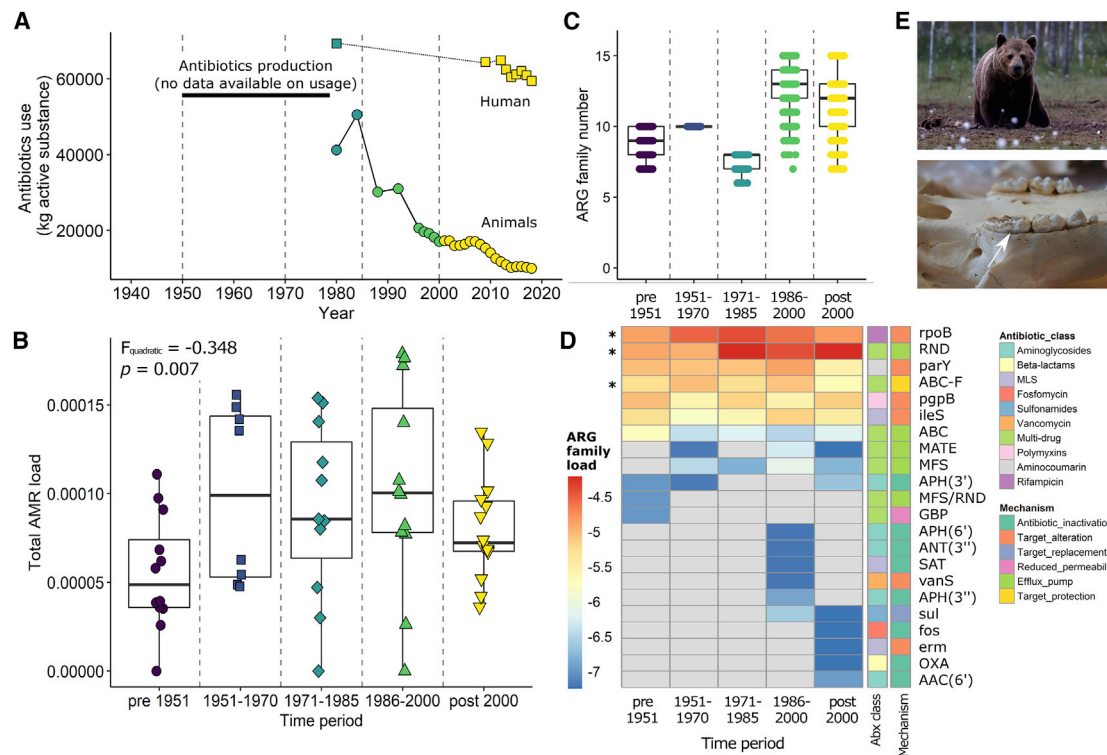


Figure 1. Total AMR load and ARG diversity in brown bear dental calculus reflect antibiotic use in Sweden

(A) Total historical antibiotic use in Sweden in humans (squares) and domesticated animals (circles), in kilograms of active substance used. Gray dashed lines indicate the five time period bins in correspondence with (B) and (C). Data points are colored by time period bin.

(B) Total AMR load in bear dental calculus samples changes through time ($n = 57$; upper left shows the effect size and p value for the quadratic term of time period from the generalized linear model, including median DNA fragment length as a co-variable; Table S1). Total AMR load was calculated as the number of reads mapping to CARD divided by the total number of oral bacterial reads in a sample. Each point within a given time period represents a unique brown bear dental calculus sample.

(C) Boxplots of the number of unique ARG families detected in each time period after subsampling to eight samples per time period (the lowest sample size available for time period 1951–1970) with 1,000 independent repeats to control for differences in sample sizes between time periods. To control for differences in the amount of data available between time periods, we also subsampled by number of reads sequenced (Figure S2).

(D) Heatmap of log-transformed ARG family loads (proportion of oral bacterial reads mapping to each ARG family) in samples pooled by time period. ARG families that were not detected in a given time period are colored gray. ARG families that significantly increased in abundance over time (either in a linear or quadratic manner) are indicated with asterisks (Table S1). ARG families are annotated by their main mechanism of resistance and the major antibiotic (abx) class to which they confer resistance, as recorded in CARD.

(E) Photo of a Scandinavian brown bear and a Scandinavian brown bear skull specimen with dental calculus (white arrow) sampled for this study (photos used with permission from Mats Björklund and Katerina Guschanski, respectively).

rpoB, rifamycin-resistant beta-subunit of RNA polymerase; *RND*, resistance-nodulation-cell division antibiotic efflux pump; *parY*, aminocoumarin-resistant topoisomerase IV; *ABC-F*, ATP-binding cassette ribosomal protection protein; *pgpB*, lipid A phosphatase; *ileS*, antibiotic-resistant isoleucyl-tRNA synthetase; *ABC*, ATP-binding cassette antibiotic efflux pump; *MATE*, multidrug and toxic compound extrusion transporter; *MFS*, major facilitator superfamily antibiotic efflux pump; *APH(3')*, phosphorylation of aminoglycoside antibiotic on the hydroxyl group at position 3'; *MFS/RND*, *MFS* and *RND* efflux pump; *GBP*, general bacterial porin with reduced permeability to beta-lactams; *APH(6')*, phosphorylation of aminoglycoside antibiotic on the hydroxyl group at position 6; *ANT(3')*, nucleotidylation of aminoglycoside antibiotic at the hydroxyl group at position 3'; *SAT*, streptothricin acetyltransferase; *vanS*, *vanS*/glycopeptide resistance gene cluster; *APH(3'')*, phosphorylation of aminoglycoside antibiotic on the hydroxyl group at position 3''; *sul*, sulfonamide-resistant *sul*; *fos*, fosfomycin thiol transferase; *erm*, Erm 23S ribosomal RNA methyltransferase; *OXA*, *OXA* beta-lactamase; *MLS*, macrolides, lincosamides, and streptogramins.

See also Figures S2 and S3 and Table S1.

mammals, including potential pathogens and ARGs.²⁴ As wide-ranging omnivores and scavengers, brown bears have a diverse diet and are exposed to potential sources of AMR from both prey species and the environment.^{4,25,26} While they generally prefer remote areas, Swedish brown bears do occasionally approach human settlements and come into contact with humans and domestic animals.^{25–27}

Here, we sequenced 82 dental calculus samples collected from museum-preserved Swedish brown bear specimens

(Figure 1) from across central and northern Sweden dating between 1842 and 2016. After read processing and rigorous quality control (Figure S1; STAR Methods), including the evaluation and removal of potential environmental contaminants,^{28,29} 57 calculus samples were retained. To minimize the possibility that estimates of AMR may be confounded by the presence of modern environmental resistant bacteria, we restricted our analysis to the subset of bacteria that are known to colonize oral cavities of humans and pets^{29–32} (Figure S1C).

Total AMR load reflects antibiotic use in Sweden

Sweden has a well-documented history of antibiotic use and control in both humans and animals. Detailed antibiotic usage data are available from 1980, 2009, and 2012–2018 (Figure 1A),^{33,34} while qualitative records report increased use from 1950 to 1980.³⁵ To determine how AMR prevalence has changed over time in brown bear oral microbial communities, we divided the sampling period into five time bins, based on qualitative and quantitative records of historical antibiotic use in Sweden and the individual's year of death: (1) pre-1951, corresponding to the pre-antibiotics era before commercial production began in Sweden;³⁶ (2) 1951–1970, when antibiotic production and use was increasing, including use of antibiotic growth promoters in livestock;^{35–37} (3) 1971–1985, when concerns about mounting AMR were first voiced but no official measures put in place;³⁸ (4) 1986–2000, when control measures were implemented, including the ban of antibiotics as growth promoters in 1986³⁴ and the Swedish strategic program against antibiotic resistance (Strama) in 1995, which regulates the sales of antibiotics for humans and animals and continuously monitors AMR;³⁹ and (5) post-2000, when the ongoing control measures in Sweden have resulted in decreased sales of antibiotics for both outpatient care and veterinary use³³ and overall low AMR prevalence compared to other European countries.⁴⁰

Total AMR load was determined by aligning the oral bacterial reads in each bear calculus sample against the Comprehensive Antibiotic Resistance Database (CARD).⁴¹ The CARD sequence with the best alignment score for each read was assigned to its respective ARG family under the Antibiotic Resistance Ontology (ARO). We detected ARGs in samples collected in the pre-antibiotics era (Figure 1B), in line with the expectation that AMR is a natural function of microbial communities, independent of contribution from human use. Our temporal analysis uncovered significant changes in total AMR load in bear calculus that followed the same general trajectory through time as inferred for antibiotic use in humans in Sweden (Figures 1A and 1B). Total AMR load increased from the 1950s through 1990s, mirroring the reported increased use of antibiotics in Sweden, before decreasing in the 2000s, following the implementation of national control measures in 1986 and 1995 (Figures 1A and 1B). Both changes in AMR load (increase and decrease) were statistically significant (generalized linear model with a quasibinomial distribution; Table S1; $p = 0.035$) and not affected by differences in DNA degradation and low sequencing depth typical for historical samples (Table S1; $p = 0.007$).

We observed a time lag of at least 15 years from the initiation of Swedish antibiotic regulation policies in 1986 to the detection of a significant decrease of AMR levels in the oral microbiome of wild brown bears post-2000. This delay was likely caused by a combination of factors, including the time required for the policies to have a measurable effect on AMR in the environment and brown bear life expectancy. Age at death was on average 5.9 years (range 1–19 years) for the specimens for whom these data were available (17 specimens, 30%), consistent with life expectancy estimates for the Swedish brown bear population (5–8 years for yearlings), which is low due to hunting.⁴² It is therefore probable that it was not until the mid-2000s that bears in our study population lived their entire lives under post-1995 Swedish antibiotic regulations.

While the contamination of natural ecosystems with human-produced antibiotics and resistant bacteria is well documented,^{7–9} our results suggest that this process may be reversible. Sweden was one of the first countries to impose legislation to control antibiotic use and today has a strong antibiotic stewardship program with thorough monitoring of resistance in human and animal populations.³⁹ The observed decrease in total AMR load in the microbiome of wild brown bears since the 2000s is mirrored by results from Swedish farm animal screening, which shows low and generally stable or decreasing resistance in *Escherichia coli* and *Staphylococcus aureus* isolates over the last 10 years.³³

Few other studies have investigated the temporal changes in AMR throughout the history of human antibiotic use. Increasing levels of AMR have been detected in archived soil samples from the 1940s to the mid-2000s.⁴³ Collections of human-associated bacteria isolated prior to 1955 have been found to have low levels of AMR,^{44,45} although other studies utilizing such collections have reported similar AMR profiles in both pre-1950s and modern strains.⁴⁶ To our knowledge, only a single study has investigated temporal changes in AMR levels in wildlife across a multi-year period, reporting increasing AMR in bacteria isolated from stranded marine mammals from 2004 to 2010.⁴⁷ Our study thus represents the first systematic quantification of AMR in wild animals over the entire history of industrial-scale human antibiotic production.

ARG diversity increases over time

The development and mass use of new antibiotic classes over the last 50 years¹ may have diversified selective pressures on naturally occurring resistant bacteria and led to a greater diversity of ARGs in wildlife microbiomes in more recent times. Thus, we characterized and quantified ARG families in bear samples across the different time periods. The overall diversity of ARG families increased from 1986 onward (Figure 1C), as reflected by the detection of novel rare ARGs (Figure 1D). This observation was not explained by differences in sample sizes (Figure 1C) or amount of data available (Figure S2) across time periods.

The mechanism of resistance tended to differ between ARG families that were consistently detected in all time periods, including in the pre-antibiotics era, and rare ARG families that were only detected in the last two time periods (Figure 1D). ARG families detected since 1986 included aminoglycoside-modifying enzymes (ANT, APH, and AAC) that target, e.g., streptomycin, and beta-lactamases (OXA) that target, e.g., penicillin.⁴⁸ Such genes are frequently encoded on plasmids and other mobile genetic elements and thus are readily transferred among different bacteria. In contrast, ubiquitous ARG families contained multidrug efflux pumps (e.g., RND), the ribosome-binding ABC-F family, and ARGs conveying AMR through alterations in antibiotic targets, such as rifamycin-resistant beta-unit of RNA polymerase (rpoB) and aminocoumarin-resistant topoisomerase IV (parY) (Figure 1D). Many of these ARGs are encoded on the chromosome and have been often co-opted for AMR as an extension of general functions related to bacterial survival.^{17,49} In support of our findings, multidrug efflux pumps, resistant rpoB, and resistant topoisomerase have been detected in microbiomes of pre-historic humans,^{23,50} providing additional evidence that these ARGs are “ancient.”⁵¹

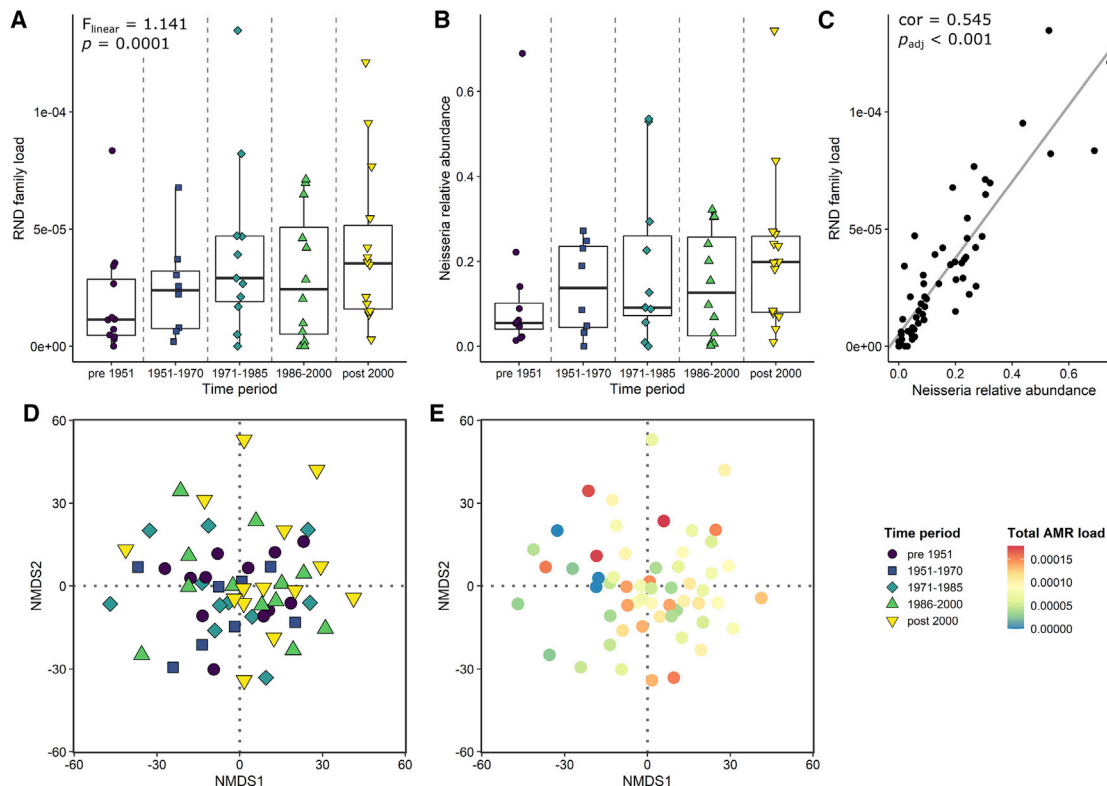


Figure 2. Changes in ARG family loads are associated with changes in abundance of oral bacterial genera over time

(A) Proportion of oral bacterial reads mapping to RND (resistance-nodulation-cell division) antibiotic efflux pump. Upper left shows the effect size and p value for the linear term of time period from the generalized linear model, including median DNA fragment length as a co-variable (Table S1). (B) Proportion of oral bacterial reads assigned by Bracken to *Neisseria* across the study time periods. (C) *Neisseria* relative abundance is correlated with RND load. Similarity score (cor) and adjusted p value (p_{adj}) from CCREPE are shown in the upper left corner of the plot. Examples of other correlations between ARG families and oral bacterial genera abundances are presented in Figure S3. (D and E) NMDS of CLR-normalized abundances of oral bacteria in bear dental calculus samples, colored by specimen time period (D) and total AMR load (E). NMDS was performed with $k = 2$ on a Euclidean distance matrix. NMDS stress: 0.188. Time period accounted for 7.38% of the variation between samples ($F_{4,52} = 1.04$, $p = 0.40$) and total AMR load accounted for 0.95% of the variation ($F_{1,55} = 0.53$, $p = 0.99$). NMDS of presence/absence of oral bacteria in bear dental calculus samples can be found in Figure S3. See also Figure S3 and Table S1.

We observed that ubiquitous ARG families changed in abundance through time (Figures 2A and S3A–S3F; Table S1). Total abundance of ABC-F and resistant *rpoB* reflected the pattern of total AMR load, increasing from 1951 to 2000 and decreasing post-2000 (Figures S3D and S3E). In contrast, the abundance of RND efflux pump consistently increased over the study period (Figure 2A). The other four most abundant ARG families (*ileS*, ABC efflux pump, *pgpB*, and *parY*; Figures S3A–S3C and S3F) showed varied abundance trajectories over time. The abundance of some ARG families was correlated with the abundance of specific oral bacterial genera (Figures S3G–S3M), e.g., RND efflux pump and *Neisseria* (Figures 2A–2C; similarity score = 0.545, $p_{adjusted} < 0.001$). *Neisseria* has a well-characterized RND system (*mtrCDE*) that exports a wide variety of antibiotics, biocides, and detergents.⁵² However, these changes in the relative abundance of specific oral genera were not reflected in the overall oral bacterial community composition at the species level, which remained stable through time (Figures 2D, 2E, S3O, and S3P). This suggests subtle responses of likely low-abundance taxa with specific AMR profiles, akin to findings in

lichen microbiomes following experimental exposure to antibiotics.⁵³

Lack of association with proximity to humans suggests widespread AMR contamination of natural environments

We hypothesized that bears found in locations close to human habitations would have higher total AMR loads, as they might be more exposed to environmental contamination from antibiotics or human-associated resistant bacteria. Fifty bear specimens had detailed information about the collection location (Figure 3A), whereas only municipality or county data were available for the remaining seven specimens. To account for human population density in the year of death and specific location of each bear, we used historical records from Swedish parishes. To estimate human impact, we used the 2009 Human Footprint Index, which combines data on human population density, land use, infrastructure, and transport networks into a single measure (Figure 3A), as no such historical data were available for the majority of specimen localities. We estimated the magnitude of human

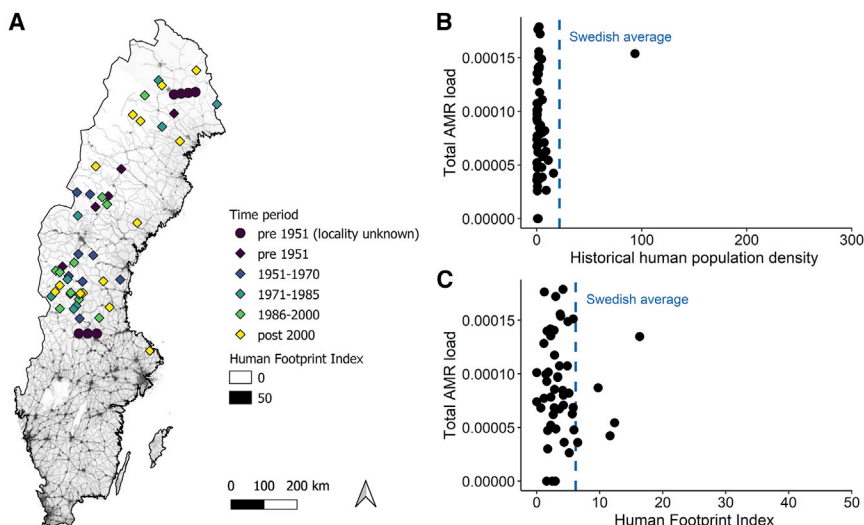


Figure 3. Total AMR load is not associated with proximity to humans or geography

(A) Geographic locations of Swedish brown bear museum specimens included in this study ($n = 57$ following filtering and processing steps). Specimens are colored by the time period in which they died and plotted according to their GPS coordinates, as obtained from museum records. Circles represent specimens without locality information, which were assigned random coordinates within their counties (seven specimens from pre-1951). No association was found between total AMR load and geographic region, including municipality and county location (Table S2). The underlying terrain of Sweden is shaded by the 2009 Human Footprint Index (higher human activities/populations correspond to darker shaded areas). The map of Sweden was obtained from Lantmäteriet (<https://www.lantmateriet.se/sv/Kartor-och-geografisk-information/geodataprodukt/produktlista/oversiktskartan>) and the Human Footprint Index data from NASA Socioeconomic Data and Applications Center (<https://doi.org/10.7927/H46T0JQ4>).

(B and C) Total AMR load compared to historical human population density per km^2 within the specimen collection locality (B) and mean Human Footprint Index within a 12.5 km radius (500 km^2) around specimen collection location (C). The majority of bear specimens were collected from areas of low human population density and low Human Footprint Indices. Dashed blue line and upper limit of the x axis correspond to average and maximum human population density of Sweden in 2000 (B) and average and maximum Human Footprint Index across Sweden (C). No association was observed between total AMR load and historical human population density or modern Human Footprint Index for any given time period (Table S1). See also Tables S1 and S2.

impact for each of the 50 bears with known location by considering an area with 12.5 km radius, which corresponds to the average brown bear home range size.⁵⁴

In contrast to our expectations, we found no association between total AMR load and historical human population density or modern Human Footprint Index (Figures 3B and 3C; Table S1), nor with geographic regions, including municipality and county location (Table S2). No association between geographic location and AMR load was observed for any given time period (Table S1). These results contrast with the frequently reported association between environmental AMR abundance and proximity to humans or human settlements. For instance, rodents residing close to livestock have been shown to have higher AMR levels compared to rodents in natural areas.^{55–58} Associations between AMR and proximity to humans have also been found in foxes, wild boars, deer, and tapirs.^{59–61} However, in contrast to these studies, the brown bear specimens considered here were generally collected from regions with low (historical) human population densities and low Human Footprint indices (Figures 3B and 3C). In addition, Swedish brown bears are solitary, were hunted almost to extinction in the 1930s,⁶² and despite population recovery, represent a low-density wildlife population with infrequent interactions with humans or livestock.²⁵

The lack of a direct link between AMR and exposure to humans suggests that the observed temporal changes in total AMR load and ARG diversity in wild bears reflect widespread contamination of natural environments that goes beyond the immediate vicinity of human habitation. Evidence exists for AMR contamination far away from the source sites. AMR of a likely anthropogenic origin has been detected in pristine environments that are expected to be free from human activities, for example, in High Arctic soils.⁶³ Migratory birds, water, and wind-blown soil particles have been suggested as important vectors for human-

associated AMR, possibly allowing for dissemination across wide distances and to remote locations.^{64,65} For example, river water and estuarine sediments contain ARGs, particularly downstream of wastewater treatment plants, livestock farms, and other anthropogenic constructions.^{7–11} Furthermore, AMR has been shown to persist in environments even in the absence of selective pressures from antibiotics. Fitness costs for maintaining AMR can be extremely variable and the strength of selection for AMR can remain constant across a large range of antibiotic concentrations, which may facilitate the maintenance of AMR in environmental microbiomes.^{66,67}

DISCUSSION

Using dental calculus, a host-associated microbiome that persists through time, we were able to quantify temporal changes in AMR load and ARG diversity from the pre-antibiotics era until the present day. Our study exemplifies how the field of ancient metagenomics can broaden our understanding of global environmental trends, including those resulting from human actions, helping us to evaluate and improve the effectiveness of environmental policies for the control of AMR. Our case study suggests that human actions, both negative and positive, can directly impact diverse microbial communities, including those associated with wild animals, and provides evidence that large-scale policies limiting the use of antimicrobials in humans and livestock may be effective in curbing the dissemination of AMR through environmentally mediated pathways.

STAR METHODS

Detailed methods are provided in the online version of this paper and include the following:

- **KEY RESOURCES TABLE**
- **RESOURCE AVAILABILITY**
 - Lead contact
 - Materials availability
 - Data and code availability
- **EXPERIMENTAL MODEL AND SUBJECT DETAILS**
- **METHOD DETAILS**
 - Sample collection
 - Sample processing and DNA extraction
 - Library preparation and sequencing
 - Data processing
 - Microbial source identification
 - Oral bacteria identification
 - Antimicrobial resistance profiling
 - Geographic and human impact data
- **QUANTIFICATION AND STATISTICAL ANALYSIS**

SUPPLEMENTAL INFORMATION

Supplemental information can be found online at <https://doi.org/10.1016/j.cub.2021.08.010>.

ACKNOWLEDGMENTS

We thank Peter Niehoff, Kevin Mulder, and Tom van der Valk for their assistance with sampling; Peter Mortensen from the Department of Zoology at the Swedish Museum of Natural History for help with specimen records and geographic coordinate conversions; Karl Pedersen from the National Veterinary Institute for advice on accessing Swedish antibiotic use data; Maria Wiselgren from the Centre for Demographic and Aging Research (CEDAR) at Umeå University for advice on accessing and navigating Swedish historical parish records; and Mats Björklund for providing a photo of a Scandinavian brown bear. Sequencing was performed by the SNP&SEQ Technology Platform in Uppsala. The facility is part of the National Genomics Infrastructure Sweden and Science for Life Laboratory. The SNP&SEQ Platform is also supported by the Swedish Research Council and the Knut and Alice Wallenberg Foundation. We also acknowledge the National Bioinformatics Infrastructure for providing computational resources to this project. We obtained geographic and human population data from a number of publicly available resources: Lantmäteriet (the Swedish mapping, cadastral, and land registration authority), SCB (Statistics Sweden), and FOLKNET (provided by CEDAR at Umeå University). This work was supported by the Formas grants 2016-00835 and 2019-00275 and the Science for Life Laboratory National Sequencing Projects grant (NP00039) to K.G.

AUTHOR CONTRIBUTIONS

Conceptualization, J.C.B. and K.G.; Methodology, J.C.B. and K.G.; Software, J.C.B.; Formal Analysis, J.C.B.; Investigation, J.C.B., H.G.L., T.H., and K.G.; Resources, D.C.K. and K.G.; Data Curation, J.C.B., D.C.K., and K.G.; Writing – Original Draft, J.C.B.; Writing – Review & Editing, J.C.B., H.G.L., T.H., D.C.K., and K.G.; Supervision, J.C.B. and K.G.; Project Administration, K.G.; Funding Acquisition, K.G.

DECLARATION OF INTERESTS

The authors declare no competing interests.

Received: June 17, 2021

Revised: July 23, 2021

Accepted: August 2, 2021

Published: August 25, 2021

REFERENCES

1. Landecker, H. (2016). Antibiotic resistance and the biology of history. *Body Soc.* 22, 19–52.
2. Naylor, N.R., Atun, R., Zhu, N., Kulasabanathan, K., Silva, S., Chatterjee, A., Knight, G.M., and Robotham, J.V. (2018). Estimating the burden of antimicrobial resistance: a systematic literature review. *Antimicrob. Resist. Infect. Control* 7, 58.
3. Thorpe, K.E., Joski, P., and Johnston, K.J. (2018). Antibiotic-resistant infection treatment costs have doubled since 2002, now exceeding \$2 billion annually. *Health Aff. (Millwood)* 37, 662–669.
4. Vittecoq, M., Godreuil, S., Prugnotte, F., Durand, P., Brazier, L., Renaud, N., Arnal, A., Aberkane, S., Jean-Pierre, H., Gauthier-Clerc, M., et al. (2016). REVIEW: Antimicrobial resistance in wildlife. *J. Appl. Ecol.* 53, 519–529.
5. Allen, H.K., Donato, J., Wang, H.H., Cloud-Hansen, K.A., Davies, J., and Handelsman, J. (2010). Call of the wild: antibiotic resistance genes in natural environments. *Nat. Rev. Microbiol.* 8, 251–259.
6. Jones, K.E., Patel, N.G., Levy, M.A., Storeygard, A., Balk, D., Gittleman, J.L., and Daszak, P. (2008). Global trends in emerging infectious diseases. *Nature* 451, 990–993.
7. Pruden, A., Arabi, M., and Storteboom, H.N. (2012). Correlation between upstream human activities and riverine antibiotic resistance genes. *Environ. Sci. Technol.* 46, 11541–11549.
8. He, L.Y., Ying, G.G., Liu, Y.S., Su, H.C., Chen, J., Liu, S.S., and Zhao, J.L. (2016). Discharge of swine wastes risks water quality and food safety: Antibiotics and antibiotic resistance genes from swine sources to the receiving environments. *Environ. Int.* 92–93, 210–219.
9. Zhu, Y.G., Zhao, Y., Li, B., Huang, C.L., Zhang, S.Y., Yu, S., Chen, Y.S., Zhang, T., Gillings, M.R., and Su, J.Q. (2017). Continental-scale pollution of estuaries with antibiotic resistance genes. *Nat. Microbiol.* 2, 16270.
10. Karkman, A., Pärnänen, K., and Larsson, D.G.J. (2019). Fecal pollution can explain antibiotic resistance gene abundances in anthropogenically impacted environments. *Nat. Commun.* 10, 80.
11. Mariano, V., McCrindle, C.M.E., Cenci-Goga, B., and Picard, J.A. (2009). Case-control study to determine whether river water can spread tetracycline resistance to unexposed impala (*Aepyceros melampus*) in Kruger National Park (South Africa). *Appl. Environ. Microbiol.* 75, 113–118.
12. Subbiah, M., Caudell, M.A., Mair, C., Davis, M.A., Matthews, L., Quinlan, R.J., Quinlan, M.B., Lyimo, B., Buza, J., Keyyu, J., and Call, D.R. (2020). Antimicrobial resistant enteric bacteria are widely distributed amongst people, animals and the environment in Tanzania. *Nat. Commun.* 11, 228.
13. Literak, I., Dolejska, M., Rybarikova, J., Cizek, A., Strejckova, P., Vyskocilova, M., Friedman, M., and Klimes, J. (2009). Highly variable patterns of antimicrobial resistance in commensal *Escherichia coli* isolates from pigs, sympatric rodents, and flies. *Microb. Drug Resist.* 15, 229–237.
14. Dolejska, M., Duskova, E., Rybarikova, J., Janoszowska, D., Roubalova, E., Dibdakova, K., Maceckova, G., Kohoutova, L., Literak, I., Smola, J., and Cizek, A. (2011). Plasmids carrying blaCTX-M-1 and qnr genes in *Escherichia coli* isolates from an equine clinic and a horseback riding centre. *J. Antimicrob. Chemother.* 66, 757–764.
15. Carlson, J.C., Hyatt, D.R., Ellis, J.W., Pipkin, D.R., Mangan, A.M., Russell, M., Bolte, D.S., Engeman, R.M., DeLiberto, T.J., and Linz, G.M. (2015). Mechanisms of antimicrobial resistant *Salmonella enterica* transmission associated with starling-livestock interactions. *Vet. Microbiol.* 179, 60–68.
16. Hibbing, M.E., Fuqua, C., Parsek, M.R., and Peterson, S.B. (2010). Bacterial competition: surviving and thriving in the microbial jungle. *Nat. Rev. Microbiol.* 8, 15–25.
17. Poole, K. (2005). Efflux-mediated antimicrobial resistance. *J. Antimicrob. Chemother.* 56, 20–51.

18. Nesme, J., Cécillon, S., Delmont, T.O., Monier, J.M., Vogel, T.M., and Simonet, P. (2014). Large-scale metagenomic-based study of antibiotic resistance in the environment. *Curr. Biol.* **24**, 1096–1100.
19. Van Goethem, M.W., Pierneef, R., Bezuidt, O.K.I., Van De Peer, Y., Cowan, D.A., and Makhalanyane, T.P. (2018). A reservoir of 'historical' antibiotic resistance genes in remote pristine Antarctic soils. *Microbiome* **6**, 40.
20. Bhullar, K., Waglechner, N., Pawlowski, A., Koteva, K., Banks, E.D., Johnston, M.D., Barton, H.A., and Wright, G.D. (2012). Antibiotic resistance is prevalent in an isolated cave microbiome. *PLoS ONE* **7**, e34953.
21. Jin, Y., and Yip, H.-K. (2002). Supragingival calculus: formation and control. *Crit. Rev. Oral Biol. Med.* **13**, 426–441.
22. Adler, C.J., Dobney, K., Weyrich, L.S., Kaidonis, J., Walker, A.W., Haak, W., Bradshaw, C.J., Townsend, G., Sołtysiak, A., Alt, K.W., et al. (2013). Sequencing ancient calcified dental plaque shows changes in oral microbiota with dietary shifts of the Neolithic and Industrial revolutions. *Nat. Genet.* **45**, 450–455.e1.
23. Warinner, C., Rodrigues, J.F.M., Vyas, R., Trachsel, C., Shved, N., Grossmann, J., Radini, A., Hancock, Y., Tito, R.Y., Fiddyment, S., et al. (2014). Pathogens and host immunity in the ancient human oral cavity. *Nat. Genet.* **46**, 336–344.
24. Brealey, J.C., Leitão, H.G., van der Valk, T., Xu, W., Bougiouri, K., Dalén, L., and Guschanski, K. (2020). Dental calculus as a tool to study the evolution of the mammalian oral microbiome. *Mol. Biol. Evol.* **37**, 3003–3022.
25. Elfström, M., Davey, M.L., Zedrosser, A., Müller, M., De Barba, M., Støen, O.G., Miquel, C., Taberlet, P., Hackländer, K., and Swenson, J.E. (2014). Do Scandinavian brown bears approach settlements to obtain high-quality food? *Biol. Conserv.* **178**, 128–135.
26. Dahle, B., Sørensen, O.J., Wedul, E.H., Swenson, J.E., and Sandegren, F. (1998). The diet of brown bears *Ursus arctos* in central Scandinavia: Effect of access to free-ranging domestic sheep *Ovis aries*. *Wildl. Biol.* **4**, 147–158.
27. Støen, O.G., Ordiz, A., Sahlén, V., Arnemo, J.M., Sæbø, S., Mattsing, G., Kristofferson, M., Brunberg, S., Kindberg, J., and Swenson, J.E. (2018). Brown bear (*Ursus arctos*) attacks resulting in human casualties in Scandinavia 1977–2016; management implications and recommendations. *PLoS ONE* **13**, e0196876.
28. Harrison, X.A., Donaldson, L., Correa-Cano, M.E., Evans, J., Fisher, D.N., Goodwin, C.E.D., Robinson, B.S., Hodgson, D.J., and Inger, R. (2018). A brief introduction to mixed effects modelling and multi-model inference in ecology. *PeerJ* **6**, e4794.
29. Mann, A.E., Sabin, S., Ziesemer, K., Vågane, Å.J., Schroeder, H., Ozga, A.T., Sankaranarayanan, K., Hofman, C.A., Fellows Yates, J.A., Salazar-García, D.C., et al. (2018). Differential preservation of endogenous human and microbial DNA in dental calculus and dentin. *Sci. Rep.* **8**, 9822.
30. Chen, T., Yu, W.H., Izard, J., Baranova, O.V., Lakshmanan, A., and Dewhirst, F.E. (2010). The Human Oral Microbiome Database: a web accessible resource for investigating oral microbe taxonomic and genomic information. *Database (Oxford)* **2010**, baq013.
31. Dewhirst, F.E., Klein, E.A., Thompson, E.C., Blanton, J.M., Chen, T., Miliella, L., Buckley, C.M.F., Davis, I.J., Bennett, M.L., and Marshall-Jones, Z.V. (2012). The canine oral microbiome. *PLoS ONE* **7**, e36067.
32. Dewhirst, F.E., Klein, E.A., Bennett, M.L., Croft, J.M., Harris, S.J., and Marshall-Jones, Z.V. (2015). The feline oral microbiome: a provisional 16S rRNA gene based taxonomy with full-length reference sequences. *Vet. Microbiol.* **175**, 294–303.
33. Folkhälsomyndigheten; National Veterinary Institute (2019). Swedres-Svarm 2018. Consumption of Antibiotics and Occurrence of Resistance in Sweden (Public Health Agency of Sweden and National Veterinary Institute).
34. Wierup, M. (2001). The Swedish experience of the 1986 year ban of antimicrobial growth promoters, with special reference to animal health, disease prevention, productivity, and usage of antimicrobials. *Microb. Drug Resist.* **7**, 183–190.
35. Begemann, S., Perkins, E., Van Hoyweghen, I., Christley, R., and Watkins, F. (2018). How political cultures produce different antibiotic policies in agriculture: a historical comparative case study between the United Kingdom and Sweden. *Sociol. Ruralis* **58**, 765–785.
36. Wickman, K. (1969). Kungl. Maj:ts proposition till riksdagen angående förvärv av aktier i AB Kabi och Apoteksvarucentralen Vitrum Apotekare AB (Sveriges Riksdag).
37. Wierup, M., Wahlström, H., and Bengtsson, B. (2021). Successful prevention of antimicrobial resistance in animals—a retrospective country case study of Sweden. *Antibiotics (Basel)* **10**, 129.
38. Edqvist, L.E., and Pedersen, K.B. (2001). Antimicrobials as growth promoters: resistance to common sense. In *Late Lessons from Early Warnings: The Precautionary Principle 1896–2000*, P. Harremoës, D. Gee, M. MacGarvin, A. Stirling, J. Keys, B. Wynne, and S.G. Vaz, eds. (European Environment Agency), pp. 100–110.
39. Folkhälsomyndigheten (2014). Swedish work on containment of antibiotic resistance, pp. 28–51.
40. Cassini, A., Högberg, L.D., Plachouras, D., Quattrocchi, A., Hoxha, A., Simonsen, G.S., Colomb-Cotinat, M., Kretzschmar, M.E., Devleeschauwer, B., Cecchini, M., et al.; Burden of AMR Collaborative Group (2019). Attributable deaths and disability-adjusted life-years caused by infections with antibiotic-resistant bacteria in the EU and the European Economic Area in 2015: a population-level modelling analysis. *Lancet Infect. Dis.* **19**, 56–66.
41. Jia, B., Raphenya, A.R., Alcock, B., Waglechner, N., Guo, P., Tsang, K.K., Lago, B.A., Dave, B.M., Pereira, S., Sharma, A.N., et al. (2017). CARD 2017: expansion and model-centric curation of the comprehensive antibiotic resistance database. *Nucleic Acids Res.* **45** (D1), D566–D573.
42. Bischof, R., Bonenfant, C., Rivrud, I.M., Zedrosser, A., Friebe, A., Coulson, T., Mysterud, A., and Swenson, J.E. (2018). Regulated hunting re-shapes the life history of brown bears. *Nat. Ecol. Evol.* **2**, 116–123.
43. Knapp, C.W., Dolfing, J., Ehlert, P.A.I., and Graham, D.W. (2010). Evidence of increasing antibiotic resistance gene abundances in archived soils since 1940. *Environ. Sci. Technol.* **44**, 580–587.
44. Smith, D.H. (1967). R factor infection of *Escherichia coli* lyophilized in 1946. *J. Bacteriol.* **94**, 2071–2072.
45. Hughes, V.M., and Datta, N. (1983). Conjugative plasmids in bacteria of the 'pre-antibiotic' era. *Nature* **302**, 725–726.
46. Fusté, E., Galisteo, G.J., Jover, L., Vinuesa, T., Villa, T.G., and Viñas, M. (2012). Comparison of antibiotic susceptibility of old and current *Serratia*. *Future Microbiol.* **7**, 781–786.
47. Wallace, C.C., Yund, P.O., Ford, T.E., Matassa, K.A., and Bass, A.L. (2013). Increase in antimicrobial resistance in bacteria isolated from stranded marine mammals of the Northwest Atlantic. *EcoHealth* **10**, 201–210.
48. Alekshun, M.N., and Levy, S.B. (2007). Molecular mechanisms of antibacterial multidrug resistance. *Cell* **128**, 1037–1050.
49. Sharkey, L.K.R., Edwards, T.A., and O'Neill, A.J. (2016). ABC-F proteins mediate antibiotic resistance through ribosomal protection. *MBio* **7**, e01975.
50. Rifkin, R.F., Vikram, S., Ramond, J.B., Rey-Iglesia, A., Brand, T.B., Porraz, G., Val, A., Hall, G., Woodborne, S., Le Bailly, M., et al. (2020). Multi-proxy analyses of a mid-15th century Middle Iron Age Bantu-speaker palaeofaecal specimen elucidates the configuration of the 'ancestral' sub-Saharan African intestinal microbiome. *Microbiome* **8**, 62.
51. D'Costa, V.M., King, C.E., Kalan, L., Morar, M., Sung, W.W.L., Schwarz, C., Froese, D., Zazula, G., Calmels, F., Debruyne, R., et al. (2011). Antibiotic resistance is ancient. *Nature* **477**, 457–461.
52. Chitsaz, M., Booth, L., Blyth, M.T., O'Mara, M.L., and Brown, M.H. (2019). Multidrug resistance in *Neisseria gonorrhoeae*: identification of functionally important residues in the MtrD efflux protein. *MBio* **10**, e02277.
53. Wicaksono, W.A., Kusstatscher, P., Erschen, S., Reisenhofer-Graber, T., Grube, M., Cernava, T., and Berg, G. (2021). Antimicrobial-specific

response from resistance gene carriers studied in a natural, highly diverse microbiome. *Microbiome* 9, 29.

54. Dahle, B., and Swenson, J.E. (2003). Home ranges in adult Scandinavian brown bears (*Ursus arctos*): effect of mass, sex, reproductive category, population density and habitat type. *J. Zool. (Lond.)* 260, 329–335.
55. Guenther, S., Grobber, M., Heidemanns, K., Schlegel, M., Ulrich, R.G., Ewers, C., and Wieler, L.H. (2010). First insights into antimicrobial resistance among faecal *Escherichia coli* isolates from small wild mammals in rural areas. *Sci. Total Environ.* 408, 3519–3522.
56. Kozak, G.K., Boerlin, P., Janecko, N., Reid-Smith, R.J., and Jardine, C. (2009). Antimicrobial resistance in *Escherichia coli* isolates from swine and wild small mammals in the proximity of swine farms and in natural environments in Ontario, Canada. *Appl. Environ. Microbiol.* 75, 559–566.
57. Nhung, N.T., Cuong, N.V., Campbell, J., Hoa, N.T., Bryant, J.E., Truc, V.N.T., Kiet, B.T., Jombart, T., Trung, N.V., Hien, V.B., et al. (2015). High levels of antimicrobial resistance among *Escherichia coli* isolates from livestock farms and synanthropic rats and shrews in the Mekong Delta of Vietnam. *Appl. Environ. Microbiol.* 81, 812–820.
58. Grall, N., Barraud, O., Wieder, I., Hua, A., Perrier, M., Babosan, A., Gaschet, M., Clermont, O., Denamur, E., Catzeffis, F., et al. (2015). Lack of dissemination of acquired resistance to β -lactams in small wild mammals around an isolated village in the Amazonian forest. *Environ. Microbiol. Rep.* 7, 698–708.
59. Skurnik, D., Ruimy, R., Andremont, A., Amorin, C., Rouquet, P., Picard, B., and Denamur, E. (2006). Effect of human vicinity on antimicrobial resistance and integrons in animal faecal *Escherichia coli*. *J. Antimicrob. Chemother.* 57, 1215–1219.
60. Cristóbal-Azkarate, J., Dunn, J.C., Day, J.M.W., and Amabile-Cuevas, C.F. (2014). Resistance to antibiotics of clinical relevance in the fecal microbiota of Mexican wildlife. *PLoS ONE* 9, e107719.
61. Mo, S.S., Urdahl, A.M., Madslie, K., Sunde, M., Nesse, L.L., Sletteaas, J.S., and Norström, M. (2018). What does the fox say? Monitoring antimicrobial resistance in the environment using wild red foxes as an indicator. *PLoS ONE* 13, e0198019.
62. Swenson, J.E., Wabakken, P., Sandegren, F., Bjärvall, A., Franzén, R., and Söderberg, A. (1995). The near extinction and recovery of brown bears in Scandinavia in relation to the bear management policies of Norway and Sweden. *Wildl. Biol.* 1, 11–25.
63. McCann, C.M., Christgen, B., Roberts, J.A., Su, J.Q., Arnold, K.E., Gray, N.D., Zhu, Y.G., and Graham, D.W. (2019). Understanding drivers of antibiotic resistance genes in High Arctic soil ecosystems. *Environ. Int.* 125, 497–504.
64. Taylor, N.G.H., Verner-Jeffreys, D.W., and Baker-Austin, C. (2011). Aquatic systems: maintaining, mixing and mobilising antimicrobial resistance? *Trends Ecol. Evol.* 26, 278–284.
65. Ahlstrom, C.A., van Toor, M.L., Woksepp, H., Chandler, J.C., Reed, J.A., Reeves, A.B., Waldenström, J., Franklin, A.B., Douglas, D.C., Bonnedahl, J., and Ramey, A.M. (2021). Evidence for continental-scale dispersal of antimicrobial resistant bacteria by landfill-foraging gulls. *Sci. Total Environ.* 764, 144551.
66. Vogwill, T., and MacLean, R.C. (2015). The genetic basis of the fitness costs of antimicrobial resistance: a meta-analysis approach. *Evol. Appl.* 8, 284–295.
67. Murray, A.K., Zhang, L., Yin, X., Zhang, T., Buckling, A., Snape, J., and Gaze, W.H. (2018). Novel insights into selection for antibiotic resistance in complex microbial communities. *MBio* 9, e00969.
68. Taylor, G.A., Kirk, H., Coombe, L., Jackman, S.D., Chu, J., Tse, K., Cheng, D., Chuah, E., Pandoh, P., Carlsen, R., et al. (2018). The genome of the North American brown bear or grizzly: *Ursus arctos* ssp. *horribilis*. *Genes (Basel)* 9, 598.
69. Schneider, V.A., Graves-Lindsay, T., Howe, K., Bouk, N., Chen, H.-C., Kitts, P.A., Murphy, T.D., Pruitt, K.D., Thibaud-Nissen, F., Albracht, D., et al. (2017). Evaluation of GRCh38 and de novo haploid genome assemblies demonstrates the enduring quality of the reference assembly. *Genome Res.* 27, 849–864.
70. Johnston, E.R., Rodriguez-R, L.M., Luo, C., Yuan, M.M., Wu, L., He, Z., Schuur, E.A.G., Luo, Y., Tiedje, J.M., Zhou, J., and Konstantinidis, K.T. (2016). Metagenomics reveals pervasive bacterial populations and reduced community diversity across the Alaska tundra ecosystem. *Front. Microbiol.* 7, 579.
71. Oh, J., Byrd, A.L., Deming, C., Conlan, S., Kong, H.H., and Segre, J.A.; NISC Comparative Sequencing Program (2014). Biogeography and individuality shape function in the human skin metagenome. *Nature* 514, 59–64.
72. Huttenhower, C., Gevers, D., Knight, R., Abubucker, S., Badger, J.H., Chinwalla, A.T., Creasy, H.H., Earl, A.M., Fitzgerald, M.G., Fulton, R.S., et al.; Human Microbiome Project Consortium (2012). Structure, function and diversity of the healthy human microbiome. *Nature* 486, 207–214.
73. Lloyd-Price, J., Mahurkar, A., Rahnavard, G., Crabtree, J., Orvis, J., Hall, A.B., Brady, A., Creasy, H.H., McCracken, C., Giglio, M.G., et al. (2017). Strains, functions and dynamics in the expanded Human Microbiome Project. *Nature* 550, 61–66.
74. Salter, S.J., Cox, M.J., Turek, E.M., Calus, S.T., Cookson, W.O., Moffatt, M.F., Turner, P., Parkhill, J., Loman, N.J., and Walker, A.W. (2014). Reagent and laboratory contamination can critically impact sequence-based microbiome analyses. *BMC Biol.* 12, 87.
75. Venter, O., Sanderson, E.W., Magrath, A., Allan, J.R., Behr, J., Jones, K.R., Possingham, H.P., Laurance, W.F., Wood, P., Fekete, B.M., et al. (2016). Global terrestrial Human Footprint maps for 1993 and 2009. *Sci. Data* 3, 160067.
76. Rohland, N., Harney, E., Mallick, S., Nordenfelt, S., and Reich, D. (2015). Partial uracil-DNA-glycosylase treatment for screening of ancient DNA. *Philos. Trans. R. Soc. Lond. B Biol. Sci.* 370, 20130624.
77. Meyer, M., and Kircher, M. (2010). Illumina sequencing library preparation for highly multiplexed target capture and sequencing. *Cold Spring Harb. Protoc.* 2010, t5448.
78. Schubert, M., Lindgreen, S., and Orlando, L. (2016). AdapterRemoval v2: rapid adapter trimming, identification, and read merging. *BMC Res. Notes* 9, 88.
79. Schmieder, R., and Edwards, R. (2011). Quality control and preprocessing of metagenomic datasets. *Bioinformatics* 27, 863–864.
80. Li, H., and Durbin, R. (2009). Fast and accurate short read alignment with Burrows-Wheeler transform. *Bioinformatics* 25, 1754–1760.
81. Li, H. (2013). Aligning sequence reads, clone sequences and assembly contigs with BWA-MEM. *arXiv*, arXiv:1303.3997. <https://arxiv.org/abs/1303.3997>.
82. Li, H., Handsaker, B., Wysoker, A., Fennell, T., Ruan, J., Homer, N., Marth, G., Abecasis, G., and Durbin, R.; 1000 Genome Project Data Processing Subgroup (2009). The Sequence Alignment/Map format and SAMtools. *Bioinformatics* 25, 2078–2079.
83. Quinlan, A.R., and Hall, I.M. (2010). BEDTools: a flexible suite of utilities for comparing genomic features. *Bioinformatics* 26, 841–842.
84. Wood, D.E., and Salzberg, S.L. (2014). Kraken: ultrafast metagenomic sequence classification using exact alignments. *Genome Biol.* 15, R46.
85. Lu, J., Breitwieser, F.P., Thielen, P., and Salzberg, S.L. (2017). Bracken: estimating species abundance in metagenomics data. *PeerJ Comput. Sci.* 3, e104.
86. Knights, D., Kuczynski, J., Charlson, E.S., Zaneveld, J., Mozer, M.C., Collman, R.G., Bushman, F.D., Knight, R., and Kelley, S.T. (2011). Bayesian community-wide culture-independent microbial source tracking. *Nat. Methods* 8, 761–763.
87. Altschul, S.F., Gish, W., Miller, W., Myers, E.W., and Lipman, D.J. (1990). Basic local alignment search tool. *J. Mol. Biol.* 215, 403–410.
88. Camacho, C., Coulouris, G., Avagyan, V., Ma, N., Papadopoulos, J., Bealer, K., and Madden, T.L. (2009). BLAST+: architecture and applications. *BMC Bioinformatics* 10, 421.

89. Oksanen, A.J., Blanchet, F.G., Friendly, M., Kindt, R., Legendre, P., Mcglinn, D., Minchin, P.R., Hara, R.B.O., Simpson, G.L., Solymos, P., et al. (2018). Vegan: Community ecology package. R package version 2.5-3. <https://CRAN.R-project.org/package=vegan>.
90. Key, F.M., Posth, C., Krause, J., Herbig, A., and Bos, K.I. (2017). Mining metagenomic data sets for ancient DNA: recommended protocols for authentication. *Trends Genet.* 33, 508–520.
91. Dabney, J., Knapp, M., Glocke, I., Gansauge, M.-T., Weihmann, A., Nickel, B., Valdiosera, C., García, N., Pääbo, S., Arsuaga, J.-L., and Meyer, M. (2013). Complete mitochondrial genome sequence of a Middle Pleistocene cave bear reconstructed from ultrashort DNA fragments. *Proc. Natl. Acad. Sci. USA* 110, 15758–15763.
92. van der Valk, T., Vezzi, F., Ormestad, M., Dalén, L., and Guschanski, K. (2020). Index hopping on the Illumina HiSeqX platform and its consequences for ancient DNA studies. *Mol. Ecol. Resour.* 20, 1171–1181.
93. Velsko, I.M., Frantz, L.A.F., Herbig, A., Larson, G., and Warinner, C. (2018). Selection of appropriate metagenome taxonomic classifiers for ancient microbiome research. *mSystems* 3, e00080.

STAR★METHODS

KEY RESOURCES TABLE

REAGENT or RESOURCE	SOURCE	IDENTIFIER
Chemicals, peptides, and recombinant proteins		
EDTA	ThermoFisher Scientific	Cat#: 15575020
Tris-HCl	ThermoFisher Scientific	Cat#: AM9855G
Tween-20	Sigma	Cat#: P9416-50ML
Proteinase K	Sigma	Cat#: P6556-25MG
Guanidine hydrochloride	Sigma	Cat#: G3272-500G
Isopropanol	Sigma	Cat#: I9516-500ML
Sodium acetate	Sigma	Cat#: S7899-500ML
PE buffer	QIAGEN	Cat#: 19065
EB buffer	QIAGEN	Cat#: 19086
Tango Buffer	ThermoFisher Scientific	Cat#: BY5
ATP	ThermoFisher Scientific	Cat#: R0441
T4 Polynucleotide Kinase	ThermoFisher Scientific	Cat#: EK0032
T4 DNA Polymerase	ThermoFisher Scientific	Cat#: EP0062
T4 DNA Ligase	ThermoFisher Scientific	Cat#: EL0011
Bst 2.0 DNA polymerase	New England Biolabs	Cat#: M0537S
PfuTurbo C _x hotstart polymerase	Agilent Genomics	Cat#: 600410
dNTP mix	ThermoFisher Scientific	Cat#: R1121
BSA	ThermoFisher Scientific	Cat#: B14
Critical commercial assays		
High Pure Viral Nucleic Acid Large Volume Kit	Roche	Cat#5114403001
MinElute PCR Purification Kit	QIAGEN	Cat#28006
AMPure XP Beads	Beckman Coulter	Cat#A63881
Maxima SYBR Green/ROX qPCR Master Mix	ThermoFisher Scientific	Cat#K0221
Qubit dsDNA HS Assay kit	ThermoFisher Scientific	Cat#Q32851
TapeStation High Sensitivity D1000 Reagents	Agilent Genomics	Cat#5067-5585
TapeStation High Sensitivity D1000 ScreenTape	Agilent Genomics	Cat#5067-5584
Deposited data		
Raw data	This study	ENA: PRJEB42014
Analyzed data	This study	https://doi.org/10.5281/zenodo.5106420
<i>Ursus arctos horribilis</i> reference genome	⁶⁸	RefSeq: GCF_003584765.1
<i>Homo sapiens</i> reference genome	⁶⁹	RefSeq: GCF_000001405.38
<i>phiX</i> reference genome		RefSeq: GCF_000819615.1
Soil metagenomes (n = 5)	⁷⁰	ENA: ERR1017187, ERR1019366, ERR1022687, ERR1034454, ERR1035437
Human skin metagenomes (n = 5)	⁷¹	SRA: SRS727524, SRS728264, SRS728285, SRS728312, SRS728355
Human gut metagenomes (n = 5)	^{72,73}	SRA: SRS011271, SRS018656, SRS019397, SRS023526, SRS051031
Human supragingival plaque metagenomes (n = 5)	^{72,73}	SRA: SRR6877300, SRR6877340, SRR6877350, SRR6877370, SRR6877399
Human medieval dental calculus metagenomes (n = 5)	²⁹	SRA: SRS015650, SRS018665, SRS018975, SRS019387, SRS023538

(Continued on next page)

Continued

REAGENT or RESOURCE	SOURCE	IDENTIFIER
Laboratory reagent metagenomes (n = 4)	⁷⁴	ENA: ERR584320, ERR584333, ERR584341, ERR584348
Comprehensive Antibiotic Resistance Database (CARD) v3.0.1	⁴¹	https://card.mcmaster.ca/download/0/broadstreet-v3.0.1.tar.gz
Swedish parish boundaries 1976-1995	Lantmäteriet	https://www.lantmateriet.se/sv/Kartor-och-geografisk-information/geodataprodukter/produktlista/socken-och-stad/
Human population data 1810-1990	N/A	http://rystad.ddb.umu.se:8090/html#/main
Human population data 2000-2015	Statistics Sweden	https://www.scb.se/vara-tjanster/oppna-data/oppna-geodata/tatorter/ ; https://www.scb.se/vara-tjanster/oppna-data/oppna-geodata/smaorter/
Human population data per county 2000	Statistics Sweden	https://www.statistikdatabasen.scb.se/pxweb/en/ssd/START_BE_BE0101_BE0101C/BefArealTathetKon/
Human Footprint data 2009	⁷⁵	https://doi.org/10.7927/H46T0JQ4
Experimental models: Organisms/strains		
82 <i>Ursus arctos arctos</i> museum specimens (dental calculus samples)	Swedish Museum of Natural History (Stockholm, Sweden)	Museum accessions available at https://doi.org/10.5281/zenodo.5106420
Oligonucleotides		
Barcoded P5 forward adaptor: 5' → 3'; CTTTCCCTACACGACGCTCTTCC GATCTxxxxxxx	CytoGene	⁷⁶
Barcoded P7 forward adaptor: 5' → 3'; GTGACTGGAGTTCAGACGTGTGCTCT TCCGATCTxxxxxxx	CytoGene	⁷⁶
Barcoded P5/P7 reverse adaptor: 5' → 3'; xxxxxxxxAGATCG	CytoGene	⁷⁶
Indexed P5 adaptor primer: 5' → 3'; AATGATACGGCGACCACCGAGATC TACACxxxxxxxACACTCTTTCCCTA CACGACGCTCTT	CytoGene	⁷⁷
Indexed P7 adaptor primer: 5' → 3'; CAAGCAGAAGACGGCATACGAGAT xxxxxxxxGTGACTGGAGTTCAGACGTGT	CytoGene	⁷⁷
preHyb qPCR forward primer: 5' → 3'; CTTTCCCTACACGACGCTCTTC	CytoGene	⁷⁶
preHyb qPCR reverse primer: 5' → 3'; GTGACTGGAGTTCAGACGTGTGCT	CytoGene	⁷⁶
IS5 qPCR P5 primer: 5' → 3'; AATGATACGGCGACCACCGA	CytoGene	⁷⁷
IS6 qPCR P7 primer: 5' → 3'; CAAGCAGAAGACGGCATACGA	CytoGene	⁷⁷
Software and algorithms		
In-house R analysis code	This study	https://doi.org/10.5281/zenodo.5106420
In-house demultiplexing and barcode trimming scripts	This study	https://doi.org/10.5281/zenodo.5106420
In-house duplicate read removal script	This study	https://doi.org/10.5281/zenodo.5106420
AdapterRemoval v2.2.2	⁷⁸	https://github.com/MikkelSchubert/adapterremoval ; RRID: SCR_011834
PrinSeq-Lite v0.20.4	⁷⁹	http://prinseq.sourceforge.net/ ; RRID: SCR_005454

(Continued on next page)

Continued

REAGENT or RESOURCE	SOURCE	IDENTIFIER
bwa mem v0.7.17	80,81	http://bio-bwa.sourceforge.net/ ; RRID: SCR_010910
SAMTools v1.9	82	http://htslib.org/ ; RRID: SCR_002105
BEDTools v2.27.1	83	https://github.com/arq5x/bedtools2 ; RRID: SCR_006646
Kraken2 v2.0.8	84	https://github.com/DerrickWood/kraken2
Bracken v2.0	85	https://github.com/jenniferlu717/Bracken
Kraken-biom	N/A	https://github.com/smdabdoub/kraken-biom
SourceTracker v1.0	86	https://github.com/danknights/sourcetracker/tree/v1.0
Blast v2.0.9+	87,88	https://ftp.ncbi.nlm.nih.gov/blast/executables/blast+/ ; RRID: SCR_004870
R v4.0.2	N/A	http://www.r-project.org/ ; RRID: SCR_001905
RStudio v1.3.959	N/A	http://www.rstudio.com/ ; RRID: SCR_000432
R package vegan	89	http://cran.r-project.org/web/packages/vegan/index.html ; RRID: SCR_011950
R package CCREPE	N/A	https://github.com/biobakery/ccrepe
QGIS v3.14.15	N/A	https://qgis.org/en/site/ ; RRID: SCR_018507

RESOURCE AVAILABILITY

Lead contact

Further information and requests for resources and reagents should be directed to and will be fulfilled by the lead contact, Katerina Guschanski (katerina.guschanski@ebc.uu.se).

Materials availability

This study did not generate new unique reagents.

Data and code availability

Shotgun metagenomic sequencing data have been deposited at the European Nucleotide Archive. The project accession number is listed in the key resources table. All original code has been deposited at Zenodo and is publicly available. DOIs are listed in the key resources table. Any additional information required to reanalyze the data reported in this paper is available from the lead contact upon request.

EXPERIMENTAL MODEL AND SUBJECT DETAILS

Dental calculus samples (n = 82) were collected from Swedish brown bear (*Ursus arctos*) specimens from the Swedish Museum of Natural History (Stockholm, Sweden). Specimen collection date (date individual died or was found dead, or date specimen arrived at the museum) ranged from 1842 to 2016. Of the 57 specimens retained for analysis, individuals were on average 5.9 years old at approximate age of death (range 1-19 years; note only 17 specimens had age at death recorded), 14 were female, 28 were male and 15 were of unknown sex.

METHOD DETAILS

Sample collection

Skulls were macroscopically examined for dental calculus deposits and evidence of oral diseases, such as caries, inflammation and ante-mortem tooth loss. We have previously observed distinct microbial communities in dental calculus samples from bear teeth with dental caries,²⁴ thus we only processed calculus deposits from teeth without macroscopic signs of oral disease. Calculus was removed from the surfaces of teeth with disposable sterile scalpel blades and deposited in sterile microcentrifuge tubes. For each individual, calculus deposits from all healthy teeth were pooled and processed as one sample. However, three individuals

were sampled twice and processed as separate samples, of which 5 samples were excluded due to low oral bacterial content. To monitor museum environmental contamination, we used a sterilized cosmetic swab to rub an interior of one bear specimen drawer for 5 s, before depositing the swab tip in a sterile microcentrifuge tube. To characterize microbial communities that colonize the external surface of museum specimens but are not oral in origin, we also swabbed the cranial surface of a bear specimen skull, keeping away from the jaw to avoid potential carryover of endogenous oral microorganisms.

The year and location at death of each individual was obtained from museum records. For 14 specimens, year of death was unknown, however we were able to confidently assign all to a time period based on museum records about the donation (e.g., year specimen was found or donated to the museum, level of decomposition of the carcass, etc). Specimen location information included county (or historical province), municipality, locality description and coordinates of where the individual was found. Coordinates were available for the majority of specimens collected after 1995 and were provided in either the RUBIN (RUtin för Biologiska INventeringar) or Swedish Grid (RT-90) system. They were converted to standard World Geodetic System 84 (WGS84) coordinates using an online converter (<http://ormbunkar.se/koordinater/>, accessed 10-10-2019). Specimens without location coordinates were assigned WGS84 coordinates by searching for the locality described in the museum record on Google Maps (<https://www.google.com/maps>, accessed 10-10-2019). Due to changing administrative boundaries over time, we then converted museum records of county/province and municipality to the modern county and municipality based on specimen coordinates. Seven specimens had unknown localities (beyond their county of origin) and were excluded from the geography and human impact analyses. However, for visualization, they are shown on the map within their known county (Figure 3A).

Sample processing and DNA extraction

All laboratory protocols were performed in a dedicated ancient DNA laboratory following stringent procedures to minimize contamination.⁹⁰ Samples were randomized to control for batch effects and extracted in batches of 16, including two blank negative controls per batch that were taken forward to library preparation. Surface decontamination of dental calculus samples, ranging in weight from < 5 mg and up to 20 mg, consisted of UV light exposure (10 min at 254 nm) followed by a wash in 500 μ l of 0.5M ethylenediaminetetraacetate (EDTA) for 1 min.²⁴ After centrifugation at 18,000 \times g for 1 min, the pellet was taken forward for DNA extraction following a silica-based method⁹¹ adapted for non-human dental calculus, as previously described.²⁴ We eluted purified DNA in 45 μ l of EB buffer (10 mM tris-hydrochloride (pH 8.0) (QIAGEN, the Netherlands) supplemented with 0.05% (v/v) Tween-20.

Library preparation and sequencing

We used a double-indexing double-barcoding approach^{76,92} during double-stranded Illumina library preparation⁷⁷ to guard against index hopping and to retain certainty about sample of origin. All primer and adaptor sequences are listed in the [key resources table](#) and sample-specific barcode-index combinations are provided at <https://doi.org/10.5281/zenodo.5106420>. We ligated adapters containing inline 7 bp barcodes⁷⁶ to both ends of the blunt-ended DNA and quantified the incomplete libraries using a quantitative PCR assay (preHyb primers in the [key resources table](#)) to estimate the number of indexing PCR cycles needed for sequencing. All extraction and library blanks were consistently lower in DNA content than the majority of samples, as measured by quantitative PCR. Samples with adaptor-ligated library concentrations similar to the blanks were excluded. Libraries were double-indexed with unique P5 and P7 indices so that each sample had a unique barcode-index combination. The first batch of indexing PCR reactions (22 samples and blanks) was performed with 18 μ l of adaptor-ligated library, 1 μ l PfuTurbo C_x hotstart polymerase (2.5 U/ μ l, Agilent Technologies, CA), 5 μ l 10X PfuTurbo C_x reaction buffer, 0.5 μ l dNTP mix (25 mM) and 1 μ l of each indexing primer (10 μ M) in 50 μ l reactions. Following optimization, the remaining indexing batches were performed with 3.2 μ l 10X PfuTurbo C_x reaction buffer and the addition of 0.09 μ l 20 mg/mL BSA (Thermo Fisher Scientific, CA). For all batches, the PCR cycling conditions were: 2 min at 95°C, 8 or 10 cycles of 30 s at 95°C, 30 s at 59°C and 1 min at 72°C, and a final step of 10 min at 72°C. Following purification with MinElute, the indexed libraries were quantified using a quantitative PCR assay⁷⁷ (IS5/IS6 primers, [key resources table](#)). We pooled 1.5 μ l of each indexed library (including blanks and swabs) and performed size selection for fragments approximately 100-500 bp in length with AMPure XP beads (Beckman Coulter, IN). The pooled library was sequenced by SciLifeLab Uppsala on 2 Illumina NovaSeq S2 flowcells using paired-end 100 bp read length v1 sequencing chemistry.

Data processing

Sequenced reads were demultiplexed and assigned to each sample with an in-house python script based on the unique combination of barcodes and indices, discarding reads with wrong barcode combinations that could be the result of index hopping.⁹² Paired-end reads that overlapped by at least 11 bp were merged, adapters and low quality terminal bases (phred scores \leq 30) were removed and trimmed and merged reads with a length < 30 bp were filtered out with AdapterRemoval v2.2.2.⁷⁸ Barcode sequences were removed from the 5' and 3' ends of merged reads with an in-house python script. All reads for each sample (i.e., across the four lanes from the two Illumina NovaSeq flowcells) were concatenated into a single file per sample. Reads with mean base quality < 30 were filtered out with PrinSeq-Lite v0.20.4.⁷⁹ Duplicate reads were removed by randomly keeping one read among those reads having an identical sequence using an in-house python script. Reads resulting from the phage PhiX spiked in during Illumina sequencing, the brown bear host and from human contamination were removed by mapping to PhiX, human⁶⁹ and grizzly bear (*U. arctos horribilis*) reference genomes⁶⁸ with bwa mem v0.7.17^{80,81} (accessions in the [key resources table](#)). We retained the unmapped reads with SAMTools v1.9⁸² and BEDTools v2.27.1⁸³ for downstream analyses.

Microbial source identification

The unmapped reads were assigned taxonomy using the *k*-mer based classifier Kraken2 v2.0.8⁸⁴ with the standard Kraken2 database (all archaea, bacteria, viruses and the human genome in RefSeq; built 2019-05-01) and default parameters. We used Kraken-biom to extract the summarized number of reads assigned at the genus and species levels. These assignments were used with SourceTracker v1.0⁸⁶ in R, to estimate the potential contribution of source microbiomes to our samples. Source sequencing reads were processed through the same pipeline as sample reads, and included soil,⁷⁰ human skin,⁷¹ human gut,^{72,73} human supragingival plaque,^{72,73} human medieval dental calculus²⁹ and laboratory reagent⁷⁴ microbiomes (accessions in the key resources table). Within SourceTracker, sample rarefaction was set to the source with the lowest summed sequencing depth (-r 20809).

Oral bacteria identification

We used Bracken v2.0⁸⁵ to estimate taxa abundances from the Kraken read assignments at the species level (-l S) using a read length of 65 bp (-r 65), a *k*-mer length of 35 bp (-k 35) and without an abundance threshold (-t 0). The data were further processed in RStudio v1.3.959 using R v4.0.2. We excluded bear calculus samples with low microbial taxa abundances (summed Bracken abundance < 12,390, corresponding to the summed Bracken abundance of the most deeply sequenced extraction blank). To reduce false-positive taxonomic assignments, we filtered out taxa present at < 0.05% relative abundance (Bracken abundance divided by sum of Bracken abundance in a sample).⁹³ We also excluded calculus samples with low proportions of taxa showing similarity to human oral microbiomes (< 5% of a sample attributed to human calculus and plaque), as estimated by SourceTracker, to remove potentially strongly contaminated samples (Figure S1). Since we were interested in endogenous AMR of the host-associated oral microbiome, we subset the dataset to a list of oral bacteria, thus excluding environmental microorganisms that may contain ARGs. To this end, we used criteria and classifications from previous dental calculus studies,^{24,29} taxa present in the Human Oral Microbiome Database³⁰ and those identified in dog and cat oral microbiota studies.^{31,32} Bracken relative abundances of oral taxa were then summarized to the genus level for some downstream analyses.

Antimicrobial resistance profiling

AMR profiling was performed as previously described.²⁴ Oral taxa reads were aligned against CARD v3.0.1 (modified 2019-02-19),⁴¹ a curated collection of resistance determinant sequences, with blast v2.0.9+^{87,88} using default parameters. Using RStudio, the DNA and Protein accession numbers associated with each CARD sequence were mapped to their respective ARO accession number and used to obtain the ARG family and resistance mechanism of each sequence. The best hit for a read was identified based on highest bit score. Where multiple hits had the same bit score, we compared the ARO terms and in all cases, the hits shared the same ARO information (ARG family and resistance mechanism). We therefore randomly chose one hit to carry forward. Total AMR load was calculated as the sum of all reads with hits in a sample, normalized by the number of sequenced oral bacteria reads. ARG family abundance was calculated as the sum of reads assigned to each ARG family in a sample normalized by the number of sequenced oral bacteria reads in that sample. We used the R package vegan,⁸⁹ function 'specnumber', to calculate ARG diversity per sample as the number of ARG families in a sample with at least one sequencing read. To obtain ARG family abundance across a time period, we calculated the sum of reads with a best hit for each ARG family in a time period (i.e., combined across samples) normalized by the number of extracted oral reads in all samples in that time period. Similarly, ARG diversity per time period was calculated as the number of ARG families in a time period with at least one sequencing read (i.e., combined across samples).

Geographic and human impact data

Historical human population data was based on publicly available Swedish church parish (församling or socken in Swedish) records. Parishes were both religious and territorial units until 1995, and recorded parish population numbers, among other details. The 50 specimens with known localities were plotted in QGIS v3.14.15 with a vector of Swedish parish boundaries as they were in the 1976-1995 Swedish property register, downloaded from Lantmäteriet, the Swedish mapping, cadastral and land registration authority (see [key resources table](#), accessed 27-05-2020). The corresponding parish for each specimen and each parish area was determined in QGIS. Publicly available historical human population data was downloaded using the FOLKNET search tool (see [key resources table](#), accessed 08-06-2020). The FOLKNET database contains the human population from each town and parish, collected every 10 years from 1810 to 1990.

Secular municipality divisions came into effect between 1971 and 1995 and the Swedish Tax Agency took over the population register in 1991. Therefore, modern human population data (for specimens collected between 1995 and 2016) was based on publicly available population statistics of Swedish towns from Statistics Sweden (SCB). ArcView GIS shape files for human population in 2000, 2010 and 2015 were downloaded and merged (see [key resources table](#), accessed 09-06-2020). Each merged vector contained the polygon boundaries and area of each town with its human population on 31st of December of the reference year. Because historical parish boundaries tended to be larger than modern town boundaries, we chose to map the modern towns to the historical parish boundaries. Thus, data from multiple towns within a parish boundary were combined. The historical parishes and corresponding modern town names, populations and areas were exported into RStudio and summed across historical parish for each reference year.

In RStudio, specimens were assigned to their closest reference year (available for each decade, e.g., a specimen with a death, found or arrival date in 1984 was assigned to the reference year 1980, while a specimen from 1985 was assigned to 1990), except for specimens collected after 2014, which were assigned to the 2015 reference year. For specimens collected before 1995, human

population was assigned as the FOLKNET historical population for the parish during the closest reference year, whereas specimens collected from 1995 were assigned human population values based on the information from SCB. Human population density (population per square kilometre) was then calculated using the area of each parish. For Figure 3B, human population density for all of Sweden and for each county in the year 2000 was downloaded from SCB (see [key resources table](#), accessed 14-12-2020).

Human activities data were not consistently available for historical time periods. We therefore used the Last of the Wild Project (version 3) 2009 Human Footprint, 2018 Release, which is a global map of the cumulative human pressure on the terrestrial environment in 2009, using eight variables (built-up environments, population density, electric power infrastructure, crop lands, pasture lands, roads, railways and navigable waterways) at a spatial resolution of approximately 1 km.⁷⁵ The GeoTiff raster file for 2009 was downloaded from the NASA Socioeconomic Data and Applications Center (accessed 04-06-2020) and imported into QGIS with the 50 specimens with assigned coordinates (visualized in Figure 3A). A 500 km² buffer zone, corresponding to a 12.5 km radius, was calculated around each specimen, corresponding to an approximate average of the home range size of adult brown bears in Sweden (100-1000 km², depending on sex and reproductive status).⁵⁴ The average Human Footprint Index was calculated within each specimen buffer zone and exported into RStudio. For Figure 3C, the average Human Footprint Index was also calculated across all of Sweden.

QUANTIFICATION AND STATISTICAL ANALYSIS

All statistical analyses were performed in RStudio. Specimen time period was treated as a five-level ordered factor for all relevant analysis. For ordination, Bracken abundance counts for all filtered taxa were normalized by the center-log ratio (CLR) transformation, using a pseudocount of 1 added to all taxa in all samples to resolve the problem of zero values. Euclidean distance matrices were calculated with the `vegdist` function. Non-metric multidimensional scaling (NMDS) was performed on the distance matrices with the `metaMDS` function (Figures 2D, 2E, and S1C). NMDS was also performed for oral bacteria on a Jaccard distance matrix calculated from binary presence/absence data (Figures S3O and S3P). Stress values and k number for each NMDS are reported in the associated figure legend. PERMANOVA was performed on distance matrices using the `adonis` function with 1000 permutations. To evaluate changes in abundance (total AMR load and ARG family abundance) over time, and/or associations with historical human population density and mean Human Footprint Index, generalized linear models (GMLs) were built with a quasibinomial distribution and a logit link function and total oral read count as weights (details and results in Table S1). To determine which potential co-variables were associated with total AMR load, continuous explanatory variables (e.g., median length of oral reads, historical human population density) were evaluated with a Spearman correlation test, while categorical variables (e.g., extraction batch, specimen county location) were evaluated with a Kruskal rank sum test (Table S2). Significant variables were included as co-variables in the generalized linear models.

ARG family diversity was calculated across specimens pooled by time period, as the number of unique ARG families detected in that time period, using the `specnumber` function. To control for different numbers of specimens between time periods, we subsampled each time period to 8 specimens (the lowest number of specimens in any time period) without replacement, using the R base function `sample`, before calculating ARG family diversity. This process was repeated 1000 times to generate a distribution of ARG family diversity values for each time period (Figure 1C). To control for differences in sequencing depth between time periods, we also subsampled each time period to 500 AMR-positive reads (the lowest number of pooled AMR-positive reads in a time period was 553), independent of specimen ID, and calculated ARG family diversity 1000 times, as above (Figure S2).

To identify correlations between ARG family abundance and bacterial genus abundance, we used the R package CCREPE (Compositionality Corrected by REnormalizaion and PERmutation), which aims to identify significant correlations between two compositional datasets while accounting for multiple hypothesis testing. We compared the four most highly abundant ARG families (ABC-F, ileS, RND and rpoB) with all oral bacterial genera, 20 bootstrap and permutation iterations and a minimum non-zero sample (subject) number per ARG family/genus of 20. For the measure of similarity (or correlation) between samples, we used CCREPE's in-built `nc.score` function, which calculates species-level co-variation and co-exclusion patterns based on an extension of Diamond's checkerboard score to ordinal data. Significantly correlated ARG-genus pairs were identified as those with $p_{\text{adjusted}} < 0.05$ (p value adjusted for multiple hypotheses with the Benjamin-Hochberg-Yekutieli procedure) and a positive correlation (i.e., `nc.score` > 0).